HAL open science

Finite Element Hodge for Spline Discrete Differential Forms. Application to the Vlasov-Poisson Equations.

Aurore Back, Eric Sonnendrücker

To cite this version:

Aurore Back, Eric Sonnendrücker. Finite Element Hodge for Spline Discrete Differential Forms. Application to the Vlasov-Poisson Equations.. 2013. hal-00822160

HAL Id: hal-00822160

https://hal.science/hal-00822160v1

Preprint submitted on 18 Jun 2013

HAL is a multi-disciplinary open access archive for the deposit and dissemination of scientific research documents, whether they are published or not. The documents may come from teaching and research institutions in France or abroad, or from public or private research centers.

L'archive ouverte pluridisciplinaire **HAL**, est destinée au dépôt et à la diffusion de documents scientifiques de niveau recherche, publiés ou non, émanant des établissements d'enseignement et de recherche français ou étrangers, des laboratoires publics ou privés.

Elsevier Editorial System(tm) for Applied Numerical Mathematics
Manuscript Draft

Manuscript Number: APNUM-D-12-00303R1

Title: Finite Element Hodge for Spline Discrete Differential Forms. Application to Vlasov-Poisson Equations

Article Type: Special Issue: NELIA 2011

Keywords: Discrete differential forms; B-splines; Vlasov-Poisson; Numerical simulation

Corresponding Author: Prof. Eric Sonnendrücker,

Corresponding Author's Institution: Max Planck Institute for Plasma Physics

First Author: Eric Sonnendrücker, PhD

Order of Authors: Eric Sonnendrücker, PhD; Aurore Back, PhD

Manuscript Region of Origin: FRANCE

Abstract: The notion of B-spline based discrete differential forms is recalled and along with a Finite Element Hodge operator, it is used to design new numerical methods for solving the Vlasov-Poisson equations.

Answer's to the referees' questions

Aurore Back and Eric Sonnendrücker

April 12, 2013

We thank the referees for the careful reading of our manuscript and for many interesting comments that helped us improve the article.

1 Answer to the questions of referee 0

1. We agree that exterior calculus is not really necessary in 1D, but this work provides a proof of principle that discrete exterior calculus tools can be applied to the simulation of Vlasov-Poisson and Vlasov-Maxwell systems. Discrete exterior calculus has been proven extremely beneficial for the simulation of the Maxwell equations and this will of course extend to the Vlasov-Maxwell equations, bringing all the benefits for Maxwell equations and in addition some very useful properties in particular for the coupling of Vlasov with Maxwell with the problem of discrete charge conservation is an important and challenging issue. This discussion has been added in the introduction.

2. The tensor product extension to higher dimensions of the Hodge operator is straightforward and present no difficulty.

3. The equivalence of Ampère and Poisson is true only in 1D. A justification is provided in the appendix.

4. Done.

5. Done.

6. Yes, section 4.1 is devoted to expressing the most important conservation properties at the continuous level in the language of differential forms. This is conservation of mass, momentum and energy. These are not automatically conserved at the discrete level even using discrete differential forms, but it can be obtained by choosing carefully the discretisation spaces and the Poisson solver with a full 2D scheme. For cost reasons, we use here a 1D splitting in which case there are no discrete conservations of momentum and energy. The discrete obtained in our framework is centred and not diffusive. This is explained.

7. Answers on numerical experiments:

   - The algorithm is mentioned for each experiment. In the first algorithm a Crank-Nicolson time integration is used at each split step. This has been added to the description of the algorithm.
   - Spline degrees have been indicated and comparisons performed.
   - The conservation properties have been better documented. Complete energy and momentum conservation is possible in a non time split setting, but this is numerically a lot more expensive and outside the scope of this paper. This will be addressed in a later paper.
   - The full linear problem is solved and the solution compared to the analytical solution of the most important mode of the linearised problem. The recurrence phenomenon does not depend on ϵ, only on δv and a fairly coarse mesh of 64 points is used in the velocity direction. Indeed the recurrence time can be explicitly computed. The formula has been added corroborating the simulation results. Also it is true that our scheme is a finite element discretisation of a transport equation which has a behaviour very similar to centred finite difference schemes. Our diagnostic comparing the numerical solution with the dominating mode of the linearised solution is a lot finer than just computing the damping rate which is included in the formula: It is the -0.1533 factor of t in the exponential. The fact that the two curves overlap until the recurrence time also proves that the damping rate is correct.
   - It has been added that a dissipation mechanism needs to be added for long time simulation. The standard algorithm has been cited.
   - Boundary conditions have been clearly defined: periodic in x and homogeneous Dirichlet in v because of compact support.
   - The conclusion has been modified.

The paper has been extensively reread and improved. We hope that it is much more accessible now.

2 Answers to the questions of referee 1

1. We have clarified the discussion on boundary conditions. The case of periodic boundary conditions is treated as if there was no boundary at all, functions leaving the domain on one side reenter it on the other. Then the knots defining the splines can be exactly be taken to be the grid points.

2. We have also precised how to choose the grid points. The grid points are chosen first, arbitrarily, but in practice we use a uniform grid. This also defines the knots for a

periodic domain and for Dirichlet conditions we first take the knots to be the grid points and then duplicate the boundary knots as many times as is needed to get the sufficient number of degrees of freedom depending on the spline degree.

3. We have detailed the presentation of the Vlasov equation.
4. This has been detailed.
5. Done.
6. The second one is correct as the background needs to be included, the first is just the contribution of the distribution function.
7. The degrees of splines are now mentioned.
8. Some energy and momentum conservation tests from the thesis are now included.
9. Page numbers are now included for the citations of the thesis

All minor errors have been corrected.

*Manuscript
Click here to view linked References

Finite Element Hodge for Spline Discrete Differential Forms. Application to the Vlasov-Poisson Equations.

Aurore Back and Eric Sonnendrücker

IRMA, Université de Strasbourg and CNRS, France,
Inria Nancy Grand Est, France

Abstract

The notion of B-spline based discrete differential forms is recalled and along with a Finite Element Hodge operator, it is used to design new numerical methods for solving the Vlasov-Poisson equations.

Keywords: Discrete differential forms, B-splines, Vlasov-Poisson, Numerical simulation.

1. Introduction

All equations describing physical phenomena can be written with differential forms in order to avoid artificial dependencies on specific coordinates system. Discrete differential forms are then a natural tool for discretising such equations. A new class of discrete differential forms based on B-splines have been introduced recently [1, 9]. This new approach has many advantages: it is easy and efficient to implement higher degree B-splines because higher degree are computed by recurrence with de Boor algorithm [13]; Discrete differential forms verify a De Rham diagram and so we have a compatible discretization with the continuous formulation; Moreover, B-splines finite elements have

gotten a lot of attention recently in the framework of isogeometric analysis [4, 9, 20]. In our previous work [1], we had constructed a finite difference Hodge for the spline discrete differential forms. In this paper we use a more classical Finite Element Hodge coming naturally from the weak formulation. We apply this numerical tool to the 1D Vlasov-Poisson equations. For this we express the Vlasov equation in the language of differential geometry. This is a first step towards a geometric discretisation of the full Vlasov-Maxwell equation. Discrete exterior calculus has been proven extremely beneficial for the simulation of the Maxwell equations (see for example [7, 17]) and this will of course extend to the Vlasov-Maxwell equations, bringing all the benefits for Maxwell equations and in addition some very useful properties, in particular for the coupling of Vlasov with Maxwell where the problem of discrete charge conservation is an important and challenging issue that has a natural geometric formulation.

The article is organised as follows. In the first part (section 2), we recall the construction of B-splines and their properties. Then, in the second one (section 3), we explain how to construct discrete differential forms as well as the discrete counterparts of the exterior derivative and the Hodge $\star$ operator [1, 7, 14, 15, 18, 17]. This last operator is different because it involves a metric. In the finite element context we use in this paper, it is natural to use a weak formulation for the discretization of Hodge star [9, 20, 18, 17]. In the last part (section 4), we apply the method on the Vlasov-Poisson equations and we get here a purely Eulerian scheme as opposed to the semi-Lagrangian generally used for this problem [12, 6, 21].

2. A short overview of B-splines

B-splines are constructed using a sequence of points which are called knots. In order to construct our spline differential forms, we first define a computational grid based on N grid points $x_1 < x_2 < \cdots < x_N$. The grid can be uniform or not. We shall consider periodic and Dirichlet boundary conditions.

For periodic boundary conditions, we can remove the boundary by using a modulo condition. Then the knot set $T = (t_i)_{1 \leqslant i \leqslant N-1}$ can be taken equal to the grid points except the last one that is not used, as knots on each side of the current knot are always well defined.

For Dirichlet boundary conditions, we use the fact that knots can be duplicated and that the spline of degree α becomes interpolating at a knot when it is replicated α times. Due to this property, Dirichlet conditions can be enforced directly on the first and last spline coefficients by replicating the boundary knots. The knots we take are then the grid points augmented by the replicated knots at each of the two boundary points. The knots define then as required a nondecreasing set of points.

Let us denote by B_i^α the B-spline of degree α (and so of order $p = \alpha + 1$) with support in the interval $[t_i, t_{i+\alpha+1}]$. Then B_i^α is defined recursively by

$$B_i^\alpha(x) = \frac{x - t_i}{t_{i+\alpha} - t_i} B_i^{\alpha-1}(x) + \frac{t_{i+\alpha+1} - x}{t_{i+\alpha+1} - t_{i+1}} B_{i+1}^{\alpha-1}(x).$$

The recursion is initialized by

$$B_i^0(x) = \chi_{[t_i, t_{i+1}[}(x), \quad \text{the characteristic function of } [t_i, t_{i+1}[.$$

The B-splines verify the following properties:

- The B-spline B_i^α is a polynomial of degree α between two consecutive knots,
- They have a linear local independance,
- If the knot t_i has a multiplicity m (where $m \leqslant p$), *i.e.* is repeated m times, the B-spline is $\mathcal{C}^{(p-m)}$ at t_i.
- Partition of unity: for any point $x \in [t_\alpha, t_{N-\alpha})$, we have $\sum_i B_i^\alpha(x) = 1$.

We shall also need the recursion formula for the derivatives:

$$B_i^{\alpha\prime}(x) = \alpha \left(\frac{B_i^{\alpha-1}(x)}{t_{i+\alpha} - t_i} - \frac{B_{i+1}^{\alpha-1}(x)}{t_{i+\alpha+1} - t_{i+1}} \right) = D_i^\alpha(x) - D_{i+1}^\alpha(x). \tag{1}$$

with $D_i^\alpha(x) = \frac{\alpha}{t_{i+\alpha}-t_i} B_i^{\alpha-1}(x)$. For details, the reader is refereed to the book of de Boor [13].

3. Construction of discrete differential forms based on B-splines

We consider a one dimensional space. The 1D mesh of our domain will be $x_1 < \cdots < x_{N-1} < x_N$. Let us denote by $\mathcal{N}$ the dimension of the B-spline space build on this mesh. As we discussed in the previous section if we consider a periodic domain, we have $\mathcal{N} = N - 1$ B-splines for any degree of splines α, and if we consider a Dirichlet boundary conditions, we have $\mathcal{N} = N + \alpha - 1$ B-splines.

In the 1D case, only the discrete 0-forms and 1-forms exist. For these two spaces, we can take the basis functions respectively as $w_i^{0,\alpha} = B_i^\alpha(x)$ and $w_i^{1,\alpha}(x) = D_i^\alpha(x)\, dx$.

The discrete space of spline 0-forms $\mathcal{W}^{0,\alpha}$ will be the vector space generated by the basis functions $w_i^{0,\alpha}$. Any function $C^0 \in \mathcal{W}^{0,\alpha}$ writes

$$C^0(x) = \sum_{j=1}^{\mathcal{N}} c_j^0 B_j^\alpha(x),$$

with the c_j^0 defined by the interpolation conditions $C^0(x_i) = \sum_{j=1}^{\mathcal{N}} c_j^0 B_j^\alpha(x_i)$ for $i = 1, ..., \mathcal{N}$.

The space of linear spline 1-forms $\mathcal{W}^{1,\alpha}$ will be the vector space generated by the basis functions $w_i^{1,\alpha}$. On a periodic domain, the number of cells is equal to the number of grid points (as the last point is identified with the first). Therefore $\bar{\mathcal{N}} := \dim \mathcal{W}^{1,\alpha} = \mathcal{N}$. In other cases $\bar{\mathcal{N}} = \mathcal{N} - 1$. Any 1-form $C^1 \in \mathcal{W}^{1,\alpha}$ writes

$$C^1(x) = \sum_{j=1}^{\bar{\mathcal{N}}} c_j^1 D_j^\alpha(x)\, dx.$$

Since 1-forms can be integrated on an 1-dimensional domain, the coefficients c_j^1 are defined by the relations

$$\int_{x_i}^{x_{i+1}} C^1(x) = \sum_{j=1}^{\bar{\mathcal{N}}} c_j^1 \int_{x_i}^{x_{i+1}} D_j^\alpha(x)\, dx \qquad \text{for } 1 \leqslant i \leqslant \bar{\mathcal{N}}.$$

For the study of these linear systems the reader is refered to the articles [13, 1, 20].

The discrete exterior derivative. The exterior derivative d is a map that associates a $(k+1)$-form to a k-form. Moreover, if we denote by $\Omega^k(\mathcal{M})$ the set of differential k-forms on $\mathcal{M}$, we have a De Rham diagram:

$$\Omega^0(\mathcal{M}) \xrightarrow{d} \Omega^1(\mathcal{M}) \xrightarrow{d} \Omega^2(\mathcal{M}) \xrightarrow{d} \Omega^3(\mathcal{M}) \dots .$$

for $\mathcal{M}$ an open star shaped domain. The discrete exterior derivative has been defined in [1, 7, 19, 18, 17]. The discrete exterior derivative is an incidence matrix containing only $1, -1$ or 0. It acts only on spline coefficients and we have the discrete De Rham diagram

$$\mathcal{W}^{0,\alpha}(\mathcal{M}) \xrightarrow{d} \mathcal{W}^{1,\alpha}(\mathcal{M}) \xrightarrow{d} \mathcal{W}^{2,\alpha}(\mathcal{M}) \xrightarrow{d} \mathcal{W}^{3,\alpha}(\mathcal{M}) \dots$$

where $\mathcal{W}^{k,\alpha}(\mathcal{M})$ represents the set of discrete k-forms with B-splines of degree α.

The discrete Hodge operator. The Hodge star operator $\star$ maps a k-form to a $(n-k)$-form where n is the dimension of the space. It requires a metric which enables to define am inner product on the space of k-forms. Then the Hodge star operator can be defined with the help of the L^2 inner product of k-forms using the relationship

$$< \omega^k, \alpha^k >= \int_{\mathcal{M}} \omega^k \wedge \star\alpha^k \quad \forall \omega^k,$$

with $\mathcal{M}$ a differential manifold, ω^k, α^k differential k-forms on $\mathcal{M}$ and $\wedge$ the wedge product operator (see [3]). This leads straightforwardly to the property that if the $(n-k)$-form γ^{n-k} is such that $\gamma^{n-k} = \star\alpha^k$ then:

$$\int_{\mathcal{M}} \omega^k \wedge \star\alpha^k = \int_{\mathcal{M}} \omega^k \wedge \gamma^{n-k} \quad \forall \omega^k. \tag{2}$$

We define the discrete Hodge star operator using the standard Galerkin procedure just replacing the continuous spaces by discrete spaces. So, given a discrete 0-form

$$C^0(x) = \sum_{j=1}^{\mathcal{N}} c_j^0 B_j^\alpha(x),$$

we define the discrete Hodge star $\star_h C^0(x)$ as the discrete 1-form $C^1(x) = \sum_{j=1}^{\bar{\mathcal{N}}} c_j^1 D_j^\alpha(x)\, dx$. Plugging these expressions directly into (2) does not yield and invertible system. Therefore we use in addition that the Hodge star operator is its own inverse for 0-forms and 1-forms in 1D. So that $\star C^1 = C^0$, and using the property that $\star dx = 1$ we get $\star C^1(x) = \sum_{j=1}^{\bar{\mathcal{N}}} c_j^1 D_j^\alpha(x)$ and using (2) in the discrete space, as the discrete 1-forms are spanned by the

basis functions $w_i^{1,\alpha} = D_i^\alpha(x)\,dx$, we get

$$\int_{\mathcal{M}} D_i^\alpha(x)\,dx \wedge \star C^1(x) = \int_{\mathcal{M}} D_i^\alpha(x)\,dx \wedge C^0(x) \quad i = 1, \ldots, \bar{\mathcal{N}}.$$

Injecting the expressions of C^0 and $\star C^1$, we obtain the following linear system, characterising the coefficients c_j^1 given c_j^0:

$$\sum_{j=1}^{\bar{\mathcal{N}}} c_j^1 \int_{\mathcal{M}} D_i^\alpha(x)\,dx \wedge D_j^\alpha(x) = \sum_{j=1}^{\mathcal{N}} c_j^0 \int_{\mathcal{M}} D_i^\alpha(x)\,dx \wedge B_j^\alpha(x).$$

In the same way, given a discrete 1-form

$$C^1(x) = \sum_{j=1}^{\bar{\mathcal{N}}} c_j^1 D_j^\alpha(x)\,dx,$$

we can define a 0-form with the form $C^0(x) = \sum_{j=1}^{\mathcal{N}} c_j^0 B_j^\alpha(x)$ such that $C^0(x)$ is an approximation of $\star C^1(x)$. Using $\omega^0 = w_i^{0,\alpha} = B_i^\alpha(x)$, we obtain the following linear system

$$\sum_{j=1}^{\bar{\mathcal{N}}} c_j^1 \int_{\mathcal{M}} B_i^\alpha(x) \wedge D_j^\alpha(x) dx = \sum_{j=1}^{\mathcal{N}} c_j^0 \int_{\mathcal{M}} B_i^\alpha(x) \wedge B_j^\alpha(x) dx.$$

To conclude, denoting by $(M_\alpha^1)_{i,j} = \int_{\mathcal{M}} D_i^\alpha(x) D_j^\alpha(x) dx$, $(S_\alpha)_{i,j} = \int_{\mathcal{M}} D_i^\alpha(x)\, B_j^\alpha(x)\,dx$, $(M_\alpha^0)_{i,j} = \int_{\mathcal{M}} B_i^\alpha(x) B_j^\alpha(x) dx$, the discrete Hodge operator which associates a 1-form to a 0-form, is represented by the matrix

$$\left(M_\alpha^1\right)^{-1} S_\alpha,$$

and the discrete Hodge operator which associates a 0-form to a 1-form, is represented by the matrix

$$\left(M_\alpha^0\right)^{-1} S_\alpha^T,$$

where S_α^T is the transpose of the matrix S_α.

We notice that, as the space of discrete 0-forms spanned by the $B_i^\alpha(x)$ does in general not have the same dimension as the space of discrete 1-forms spanned by the $D_i^\alpha(x)\,dx$, S_α is not a square matrix (except for periodic boundary conditions) as opposed to M_α^1 and M_α^0 which are always nonsingular (see [20, 9]).

Now, we will see that the construction of the Hodge star operator in higher dimensions is just a tensor product construction of these matrices by definition of 3D discrete differential forms.

Extension to higher dimensions. Higher dimensional discrete differential forms can be derived from the one dimensional case using a tensor product construction. For example the 3D discrete differential forms will be defined as the span of the following basis functions:

- The basis functions for the 0-forms are

$$ {}^0w_{i,j,k}^\alpha(x,y,z) = B_i^\alpha(x)B_j^\alpha(y)B_k^\alpha(z). $$

- The basis functions for the 1-forms are

$$ \begin{aligned} {}^1\mathbf{w}_{i,j,k}^{\alpha,x}(x,y,z) &= D_i^\alpha(x)B_j^\alpha(y)B_k^\alpha(z)\,dx, \\ {}^1\mathbf{w}_{i,j,k}^{\alpha,y}(x,y,z) &= B_i^\alpha(x)D_j^\alpha(y)B_k^\alpha(z)\,dy, \\ {}^1\mathbf{w}_{i,j,k}^{\alpha,z}(x,y,z) &= B_i^\alpha(x)B_j^\alpha(y)D_k^\alpha(z)\,dz. \end{aligned} $$

- The basis functions for the 2-forms are

$$
\begin{aligned}
{}^2\mathbf{w}^{\alpha,x}_{i,j,k}(x,y,z) &= B^\alpha_i(x)D^\alpha_j(y)D^\alpha_k(z)\,dy\wedge dz,\\
{}^2\mathbf{w}^{\alpha,y}_{i,j,k}(x,y,z) &= D^\alpha_i(x)B^\alpha_j(y)D^\alpha_k(z)\,dz\wedge dx,\\
{}^2\mathbf{w}^{\alpha,z}_{i,j,k}(x,y,z) &= D^\alpha_i(x)D^\alpha_j(y)B^\alpha_k(z)\,dx\wedge dy.
\end{aligned}
$$

- The basis functions for the 3-forms are

$$
{}^3w^\alpha_{i,j,k}(x,y,z) = D^\alpha_i(x)D^\alpha_j(y)D^\alpha_k(z)\,dx\wedge dy\wedge dz.
$$

This construction will yield the same basis functions as in [9, 10] and [20] where vector calculus is used. The matrices allowing to compute the coefficients of B-splines in 3D are just the tensor product of 1D matrices and for the Hodge star operator in higher dimensions it is just the inverse matrix of the tensor product of 1D matrices, M_α applied on the tensor product of 1D matrices, S_α.

4. Application to Vlasov-Poisson's equations

4.1. Theory in 1D

The Vlasov equation describes the evolution in time of the distribution function $f \equiv f(x,v,t)$ of a collection of charged particles on a periodic domain of period L in x and on the whole line $]-\infty,+\infty[$ in v. It depends on position x, velocity v and time t. It reads

$$
\frac{\partial f}{\partial t} + v\frac{\partial f}{\partial x} + E(x,t)\frac{\partial f}{\partial v} = 0, \tag{3}
$$

where $E(x,t)$ is the electric field that we will consider here to be only the self-consistent field generated by the particles. Then the Vlasov equation is coupled with an equation giving the self-consistent electric field E, which can be either the Ampère equation

$$\frac{\partial E}{\partial t} = -J(x,t) = -\int f(x,v,t)v\,dv. \tag{4}$$

or the Poisson equation

$$\frac{\partial E}{\partial x} = \rho(x,t) - \rho_0 \tag{5}$$

where $\rho(x,t) = \int f(x,v,t)\,dv$ and ρ_0 is a constant describing the neutralising background which is defined by $\rho_0 = \frac{1}{L}\int_0^L \int f_0(x,v)\,dx\,dv$, so that the total charge in the domain vanishes. Here $f_0(x,v) = f(x,v,0)$ denotes the initial condition.

We can prove that the Vlasov-Ampere equation or the Vlasov-Poisson equation are equivalent in 1D (see Appendix A), provided the initial electric field is compatible with the initial density and the initial current density $J(x,0)$ is of 0 average. This is not true in higher dimensions, where the magnetic field appears in Ampère's equation.

We can write these equations using differential forms. Note that the distribution function f is defined in the two dimensional phase-space and the electric field, charge and current densities are one dimensional. We will thus need both differential forms in 2D and 1D. We choose to define the distribution function $\mathbf{f}^0$ as a 0-form in the two dimensional phase space, the electric field $\mathbf{E}^1$ as 1-form and the electric displacement $\mathbf{D}^0$ as a 0-form in the one dimensional physical space. We have $\star\mathbf{D}^0 = \mathbf{E}^1$ (given by the constitutive equations) and $d\mathbf{E}^1 = 0$ (given by Faraday equation for a null

magnetic field). We deduce that the electric field is an exact form and so it exists a 0-form (the electric potential) denoted by ϕ^0 such as $d\phi^0 = \mathbf{E}^1$ (since $\star\mathbf{D}^0 = \mathbf{E}^1$ we obtain $\star\mathbf{D}^0 = d\phi^0$). On the other hand the Vlasov equation becomes:

$$\frac{\partial \mathbf{f}^0}{\partial t} + v\frac{\partial \mathbf{f}^0}{\partial x} + i_{\frac{\partial}{\partial x}} E^1 \frac{\partial \mathbf{f}^0}{\partial v} = 0.$$

where i_τ represents the interior product along the vector field τ [3]. An other option would be to consider f as a 2-form. See [2], p. 128 and following for details. The interior product of a 1-form ω with a vector τ is the 0-form defined by $i_\tau\omega = \omega(\tau)$ for any vector v. On the other hand the Ampere and Poisson equations become

$$\begin{aligned} \frac{\partial\, \mathbf{D}^0}{\partial t} &= -\mathbf{J}^0, \\ d\,\mathbf{D}^0 &= \rho^1, \end{aligned}$$

where $\rho^1 = \int_v \star\mathbf{f}^0 - \star_x \rho_0$ is a 1-form and $\mathbf{J}^0$ a 0-form.

Let us recall conservation of mass and total momentum of the Vlasov equation using the language of differential forms. More details can be found in [2] on page 4 to 11:

Conservation of mass. We observe that if we integrate the Hodge star of Vlasov equation over phase space, we obtain the conservation of mass:

$$\frac{\partial}{\partial t}\int_{\mathcal{M}}\int_v \star\mathbf{f}^0 = 0.$$

The conservation of momentum. To find the conservation of momentum, we do the interior product along the vector field $\tau_x = v\frac{\partial}{\partial x}$ of the Hodge star of Vlasov equation then we integrate it over phase space. We obtain

$$\frac{\partial}{\partial t} i_{\tau_x}\mathbf{f}^2 + i_{\tau_x} d i_{v\frac{\partial}{\partial x}}\,\mathbf{f}^2 + i_{\tau_x} d i_{\mathbf{D}^0\frac{\partial}{\partial v}}\,\mathbf{f}^2 = 0. \tag{6}$$

with $\mathbf{f}^2 = \star\mathbf{f}^0$. We observe that this equation is on a 1-form so in order to integrate it over the 2D phase space we do the wedge product with a Killing form u (which means that u conserves the metric) and after we can integrate over phase space. We obtain, after simplification:

$$\frac{\partial}{\partial t}\int_{\mathcal{M}} \mathbf{J}^0 \wedge u = 0, \tag{7}$$

where u can be equal to dx.

Conservation of energy. For the conservation of energy we must do the wedge product between the Hodge star of Vlasov equation and $v^2 = \star(v \wedge \star v)$ then we integrate it over the space phase. We obtain

$$\frac{\partial}{\partial t}\int \star(v \wedge \star v) \wedge \mathbf{f}^2 - 2\int_{\mathcal{M}} \mathbf{J}^0 \wedge \mathbf{E}^1 = 0 \tag{8}$$

But the wedge product between the Ampre equation and $\mathbf{E}^1$ give us

$$\frac{\partial\, \mathbf{D}^0 \wedge \mathbf{E}^1}{\partial t} = -2\, \mathbf{J}^0 \wedge \mathbf{E}^1.$$

So we deduce the following conservation of energy:

$$\frac{\partial}{\partial t}\left(\int \star(v \wedge \star v) \wedge \mathbf{f}^2 + \int_{\mathcal{M}} \mathbf{D}^0 \wedge \mathbf{E}^1\right) = 0. \tag{9}$$

4.2. Numerical algorithm

We consider the 1D Vlasov-Poisson equations on a periodic domain $[0, L]$ in x and infinite in v (but as the distribution function has an exponential decay in velocity we can restrict the velocity domain for the numerical computations to the interval $[-A, A]$ with A large enough so that f is 0 up to round-off error at $\pm A$). We consider the distribution function $\mathbf{f}^0$, the electric field $\mathbf{D}^0$ and the potential ϕ^0 as 0-forms so their discrete formulations are

$$\mathbf{f}^0(x, v, t) = \sum_{i,j} f^0_{i,j}(t) B^\alpha_i(x)\, B^\alpha_j(v), \qquad \mathbf{D}^0(x, t) = \sum_i d^0_i(t) B^\alpha_i(x),$$

and

$$\phi^0(x,t) = \sum_i \phi_i^0(t) B_i^\alpha(x).$$

We also suppose that the density ρ^1 and the electric field $\mathbf{E}^1$ are 1-forms in x:

$$\rho^1(x,t) = \sum_i \rho_i^1(t) D_i^\alpha(x)\, dx \quad \text{and} \quad \mathbf{E}^1(x,t) = \sum_i e_i^1(t) D_i^\alpha(x)\, dx.$$

Their coefficients will be defined with the help of the techniques introduced in the section 3.

Classically the Vlasov-Poisson equations are solved using an operator splitting method. This has been done in [2] page 127 using a weak formulation or a finite element method at every stage. Not that the splitting method does not enable to get the exact numerical conservation of momentum and energy. The method consists in decomposing the Vlasov-Poisson equations in two parts:

- an advection in x where v is fixed

$$\frac{\partial \mathbf{f}^0}{\partial t} + v \frac{\partial \mathbf{f}^0}{\partial x} = 0, \tag{10}$$

- an advection in v where x is fixed

$$\frac{\partial \mathbf{f}^0}{\partial t} + i_{\frac{\partial}{\partial x}} E^1 \frac{\partial \mathbf{f}^0}{\partial v} = 0. \tag{11}$$

Initialisation. The distribution function $\mathbf{f}^0(0,x,v)$ is projected onto the finite element space using a L^2 orthogonal projection. Then, we compute

$$\rho^1(x,0) = \sum_i \rho_i^1(0) D_i^\alpha(x) dx,$$

such that $\rho^1 = \int_v \star\mathbf{f}^0 - \star_x\rho_0$ ($\star_x$ represents the Hodge star in x). For doing this, we use the definition of the discrete Hodge star in x. We denote by

$$\star_x\mathbf{f}_x^0(0,x) := \int_v \star\mathbf{f}^0 = \int_v \sum_{i,j} f_{i,j}^0(0) B_i^\alpha(x)\, B_j^\alpha(v) dx dv = \sum_i f_{x,i}^0(0) B_i^\alpha(x)\, dx.$$

So $\rho^1 = \star_x(\mathbf{f}_x^0(0,x) - \rho_0)$ and the spline coefficients of ρ^1, ρ_i^1 are obtained when we apply the wedge product between $\star\rho^1$ and $D_i^\alpha(x)dx$ and we integrate it over $\mathcal{M}$:

$$\rho^1 = \left(M_{\alpha,x}^1\right)^{-1} S_\alpha(f_x^0 - \rho_0),$$

with f_x^0 the spline coefficients of $\star_x\mathbf{f}_x^0$.

Then we solve the Poisson equation $d\,\mathbf{D}^0 = \rho^1$ with the help of $\int_x \star\mathbf{D}^0 = 0$. Moreover, since $\star\mathbf{D}^0 = \mathbf{E}^1$ and $d\phi^0 = \mathbf{E}^1$, we compute the spline coefficients $\mathbf{e}^1$ of $\mathbf{E}^1$ i.e.

$$\mathbf{e}^1 = \left(M_{\alpha,x}^1\right)^{-1} S_\alpha \mathbf{d}^0,$$

to have the spline coefficients ϕ_i^0 of ϕ^0 such that $d\phi^0 = \mathbf{E}^1$.

We have implemented two different time stepping algorithms, both based on a second order Strang-splitting scheme. Let us describe the steps enabling in each case to go from time t_n to time t_{n+1}.

Algorithm 1. We suppose that we know the spline coefficients of $\mathbf{f}^0(t_n)$ and $\mathbf{D}^0(t_n)$.

First, we solve with a time step $\Delta t/2$ and with a time scheme of order 2 (Crank-Nicolson), the equation

$$\frac{\partial f}{\partial t} + \mathbf{D}^0(t_n)\frac{\partial f}{\partial v} = 0,$$

using a weak formulation. We obtain an equation on spline coefficients:

$$\frac{\partial}{\partial t} M_\alpha^0(v) f^0 M_\alpha^0(x) + P_{\alpha,v} f^0 D_\alpha = 0,$$

with

$$(P_{\alpha,v})_{i,j} = \left(\int_v B_i^\alpha(v)(B_j^\alpha)'(v)dv\right) \quad \text{and} \quad (D_\alpha)_{i,j} = \left(\int_x B_i^\alpha(x)\mathbf{D}^0(t_n)B_j^\alpha(x)dx\right).$$

Then, we solve with a time step Δt and with a time scheme of order 2 (Crank-Nicolson), the equation

$$\frac{\partial f}{\partial t} + v\frac{\partial f}{\partial x} = 0,$$

using a weak formulation. We obtain an equation on spline coefficients:

$$\frac{\partial}{\partial t}M_\alpha^0(v)f^0M_\alpha^0(x) + V\, f^0\, {}^tP_{\alpha,x} = 0,$$

with ${}^tP_{\alpha,x}$ the transposed matrix and

$$V_{i,j} = \left(\int_v B_i^\alpha(v)\, v\, B_j^\alpha(v)dv\right).$$

Now, we can deduce the new spline coefficients for ${}^1\rho(t_{n+1})$ and for $\mathbf{D}^0(t_{n+1})$ by solving the Poisson equation.

For, the last stage we solve again with a time step $\Delta t/2$ and with a time scheme order 2, the equation

$$\frac{\partial f}{\partial t} + \mathbf{D}^0(t_{n+1})\frac{\partial f}{\partial v} = 0.$$

We propose another manner to solve these equations. We use also the splitting but instead of doing the finite element in two direction in each time step, we fixed a point and we apply the weak formulation in the other direction. For example, for the advection in the direction x, for all point v_l in our mesh we apply on the equation the wedge product by $B_k^\alpha(x)dx$ and we integrate it over space. Then, we resolve it in time with help of the ETD method (Exponential Time differencing) and so that is avoided to have the CFL condition on the time step. This method is explained in details on [2] page 144. The algorithm is

Algorithm 2. We suppose that we know the spline coefficients f^n of $\mathbf{f}^{0,n} = \mathbf{f}^0(t_n)$ and $\phi^{0,n} = \phi^0(t_n)$.

- First, we solve, on a half time step $\Delta t/2$ and using the ETD method of Cox and Matthews [11], the advection in v of the Vlasov equation (10), with a weak formulation in v (i.e. doing on the equation the wedge product by $B_l^\alpha(v)dv$ and integrating it over velocity space). We obtain an equation on the spline coefficients for each point x_k of our mesh:

$$f^*(t_{n+1/2}, x_k) = \exp\left(-\frac{\Delta t}{2}\mathbf{D}^0(x_k, t_n)(M^0_{\alpha,v})^{-1}P_{\alpha,v}\right)f^*(t_n, x_k),$$

  where the vector $f^*(t_n, x_k)$ is equal to $\sum_i f^0_{i,j}(t_n)B_i^\alpha(x_k)$. Then we compute the new spline coefficients $f^0_{i,j}(t_{n+1/3}) = N^{-1}_{\alpha,x}f^*(t_{n+1/2}, x_k)$ where $(N_{\alpha,x})_{i,j} = B_i^\alpha(x_j)$.

- Then, we solve, on a time step Δt and using the ETD method, the advection in x of the Vlasov equation (11), with a weak formulation in x (i.e. doing on the equation the wedge product by $B_k^\alpha(x)dx$ and integrating it over space). We obtain an equation on spline coefficients for each point v_l of our mesh:

$$f^{**}(t_{n+1}, v_l) = \exp\left(-\Delta t\, v_l\, (M^0_{\alpha,x})^{-1t}P_{\alpha,x}\right)f^{**}(t_n, v_l),$$

  where the vector $f^{**}(t_n, v_l)$ is equal to $\sum_j f^0_{i,j}(t_{n+1/3})B_j^\alpha(v_l)$. Then we compute the new spline coefficients $f^0_{i,j}(t_{n+2/3}) = N^{-1}_{\alpha,v}f^{**}(t_{n+1}, v_l)$ where $(N_{\alpha,v})_{i,j} = B_i^\alpha(v_j)$.

- Then, we can deduce $\rho^1(t_{n+1})$ from $f^0_{i,j}(t_{n+2/3})$ and solving the Poisson equation with the procedure explained previously we obtain $\mathbf{D}^0(t_{n+1})$ and also $\phi^0(t_{n+1})$.

- Finally, we solve again, on a half time step $\Delta t/2$ and using the ETD method, the advection in v of the Vlasov equation (10), with a weak formulation in v. We obtain an equation on spline coefficients for each points x_k:

$$f^*(t_{n+1}, x_k) = \exp\left(-\frac{\Delta t}{2}\mathbf{D}^0(x_k, t_{n+1})(M^0_{\alpha,v})^{-1}P_{\alpha,v}\right)f^*(t_{n+1/2}, x_k),$$

  where the vector $f^*(t_{n+1/2}, x_k)$ is equal to $\sum_i f^0_{i,j}(t_{n+2/3})B^\alpha_i(x_k)$. Then we compute the new spline coefficients $f^0_{i,j}(t_{n+1}) = N^{-1}_{\alpha,x}f^*(t_{n+1}, x_k)$.

Note that both schemes amount to using a Finite Element discretisation in phase space of the transport problem with no unwinding mechanism. This is unstable for long time computations, but can be easily stabilised adding some viscosity which would be artificial collisions in our case. See the corresponding section for the Arakawa scheme in [16] for details.

4.3. Numerical results

We consider the Vlasov-Poisson 1D with a distribution function for the electrons and neutralizing ion background on a periodic domain $[0, L]$ in x and an infinite domain in v. For the simulation, we truncate the velocity space to a segment $[-A, A]$ such that during the whole simulation, ${}^0f$ stays around round-off error for velocities close to $-A$ or A. We define an uniform mesh of the phase space $x_i = \frac{iL}{N}$, for $i = 0, \ldots, N-1$ ($x_N = x_0$ by periodicity) and $v_j = -A + \frac{j2A}{M}$, for $j = 0, \ldots, M$. The boundary condition imposed in v in the simulation is then the Dirichlet boundary condition $f(x, \pm A) = 0$ and periodic boundary conditions in x. When nothing is mentioned splines of degree 3 are used for the simulations, but comparisons between degree 1, 3 and 5 will also be presented.

4.3.1. Landau Damping

The Landau Damping problem corresponds to the initial condition

$$f^0(x,v,0) = (1+\epsilon\,\cos(k\,x))\frac{1}{\sqrt{2\pi}}\exp\left(-\frac{v^2}{2}\right),$$

with $(x,v) \in [0,L]\times[-10,10]$ where $L = \frac{2\pi}{k}$. The classical solution of the linearized Vlasov-Poisson around the maxwellian equilibrium yields for $k = 0.5$ the least damped part of the electric field

$$\mathbf{D}^0(x,t) = 4\,\epsilon\,0.3677\exp\left(-0.1533t\right)\sin(0.5x)\cos(1.4156t - 0.536245).$$

We take $\epsilon = 0.001$ and with 64 points in x and in v we compare the conservation of different physic quantities. First the solution of the linearized system is well recovered and the results are undistinguishable for our two methods. The traditional decay of the electric energy can be observed on Figure 1. We also observe the classical recurrence phenomenon due to the uniform velocity grid. An approximate formula for the recurrence time is given in [22]. It is $T_R = L/\Delta v$, where L is the period in x. In our case, $L = 4\pi$ and $\Delta v = 0.3125$, so that $T_R \approx 40.2$ which corresponds to the observed recurrence time.

Our algorithm conserves mass, which is verified numerically, mass being conserved up to round-off error for all methods. Momentum, energy and L^2 norm are exactly conserved by none of the two methods but still with a very good numerical accuracy for this problem. Figures 2, 3, 4 and 5 show the time evolution of energy and momentum for the two algorithms and different spline degrees. These conservation properties depend on the perturbation parameter ϵ and get a little bit worse but still good for larger values of ϵ. This values are not relevant for the Landau damping problem. The conservation

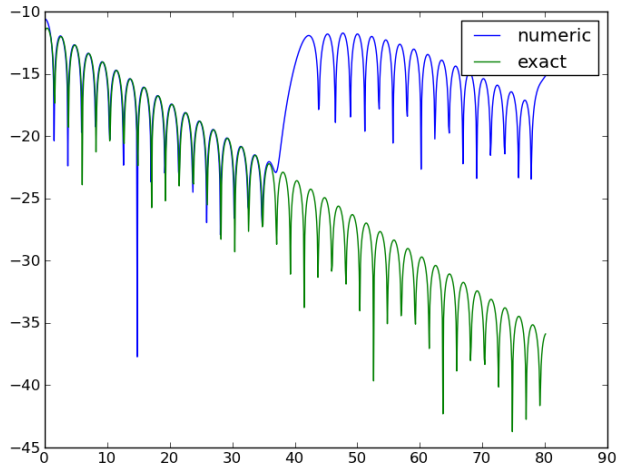

Figure 1: Log of potential energy versus time for Landau damping.

properties when the physics is further away from equilibrium will be evaluated in the next test case.

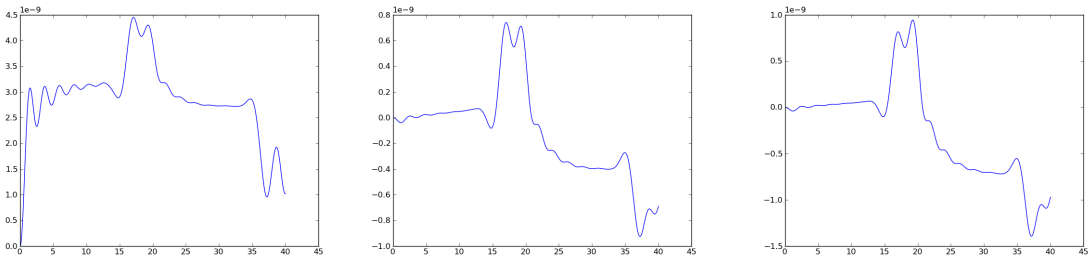

Figure 2: The relative error of energy with the first algorithm and for different degree of spline and for $\epsilon = 0.001$. To the left to right the degree of spline is equal to $1, 3$ and 5.

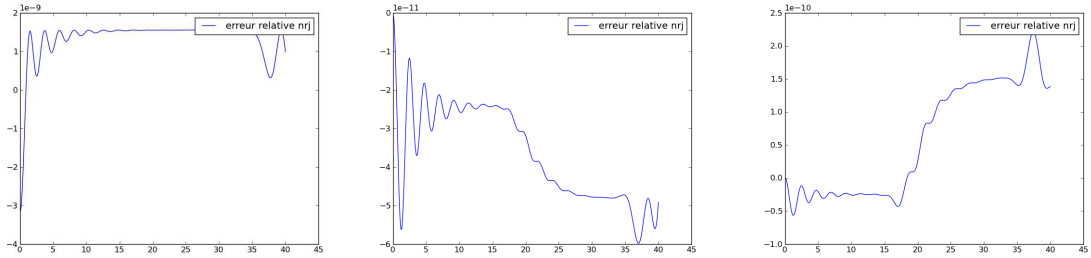

Figure 3: The relative error of energy with the second algorithm and for different degree of spline and for $\epsilon = 0.001$. To the left to right the degree of spline is equal to $1, 3$ and 5.

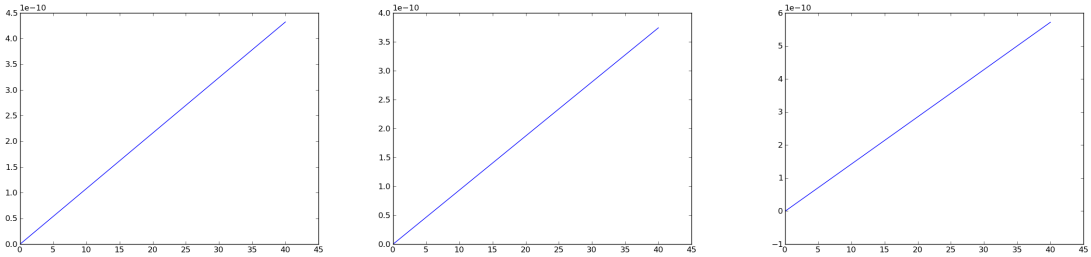

Figure 4: The relative error of momentum with the first algorithm and for different degree of spline and for $\epsilon = 0.001$. To the left to right the degree of spline is equal to $1, 3$ and 5.

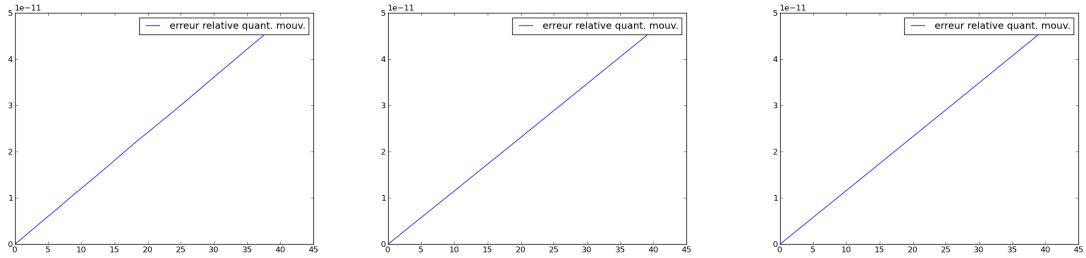

Figure 5: The relative error of momentum with the second algorithm and for different degree of spline and for $\epsilon = 0.001$. To the left to right the degree of spline is equal to $1, 3$ and 5.

4.3.2. Two stream instability

The two stream instability is generated by two beams moving with opposite velocities. This configuration can be stable or unstable depending on the value of the velocity. We consider here an unstable case for which the initial condition is

$$f^0(x,v,0) = \frac{1}{6\sqrt{2\pi}}(1+5\,v^2)\exp\left(-0.5v^2\right)(1+\epsilon\,(\cos(k\,x)+\frac{(\cos(2\,k\,x)+\cos(3\,k\,x))}{1.2})),$$

with $(x,v) \in [0,L]\times[-6,6]$ where $L = \frac{2\pi}{k}$. In the simulation we take $k = 0.2$ and $\epsilon = 0.01$. We take a time step $\Delta t = 0.01$ and 128 points in both x and v-directions.

The evolution of the distribution function in time is represented in Figure 6. We see the generation of two vortices that merge at later time so that only one survives at the end. This corresponds to what is expected. One other observation is that compared to standard simulations which include a dissipative mechanism, like cubic splines or WENO, the distribution function becomes noisy at late times. This is reminiscent of schemes conserving exactly the L^2 norm like the Arakawa scheme. An explicit dissipation mechanism needs to be added in this case. See [16] for more details.

Note that apart from mass which is conserved exactly by the algorithm, the different conserved quantities are conserved approximately but with a very good accuracy as long as the fine scales are well resolved on the grid. Figure 7 and the following support this statement. Note that mass conservation is not completely up to round-off errors as for the Landau damping test case. This is because the velocity boundary has been chose smaller, so that we lose a little bit of mass at the boundary.

An algebraically exact conservation could be achieved with spline discrete

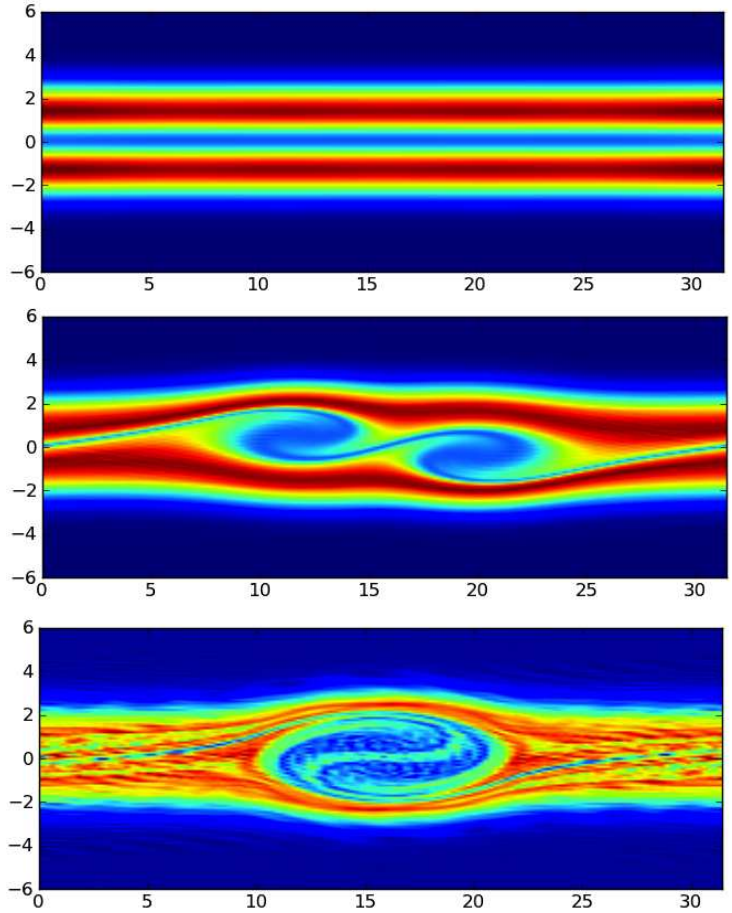

Figure 6: Snapshots of the distribution function at different times

differential forms provided no splitting is performed as the two terms need to balance each other exactly for energy conservation, which is impossible to achieve with a split-step method.

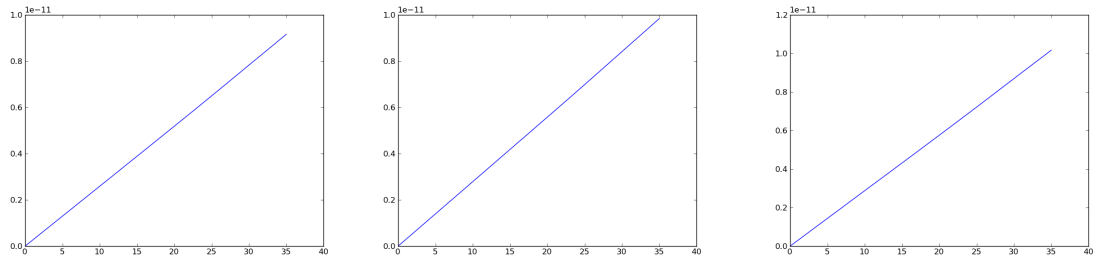

Figure 7: The relative error of mass for different degree of spline and with the first algorithm. To the left to right the degree of spline is equal to $1, 3$ and 5.

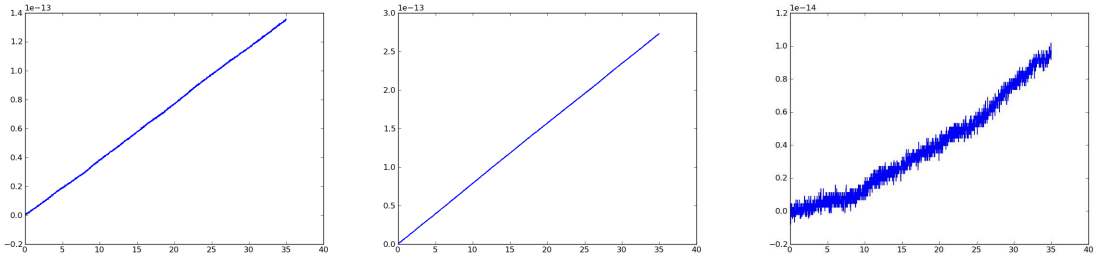

Figure 8: The relative error of mass for different degree of spline and with the second algorithm. To the left to right the degree of spline is equal to $1, 3$ and 5.

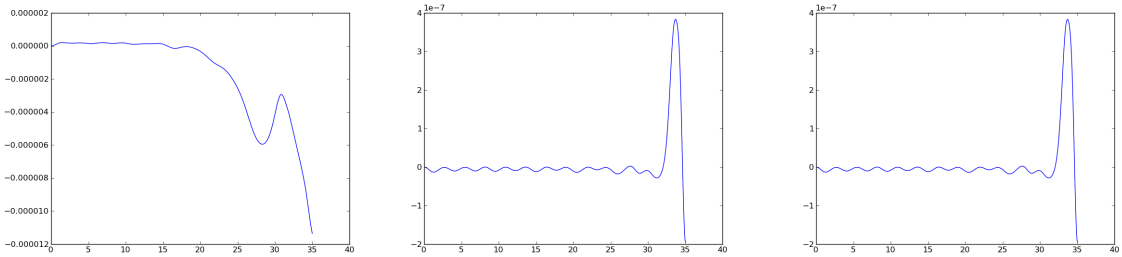

Figure 9: The relative error of energy for different degree of spline with the first algorithm. To the left to right the degree of spline is equal to $1, 3$ and 5.

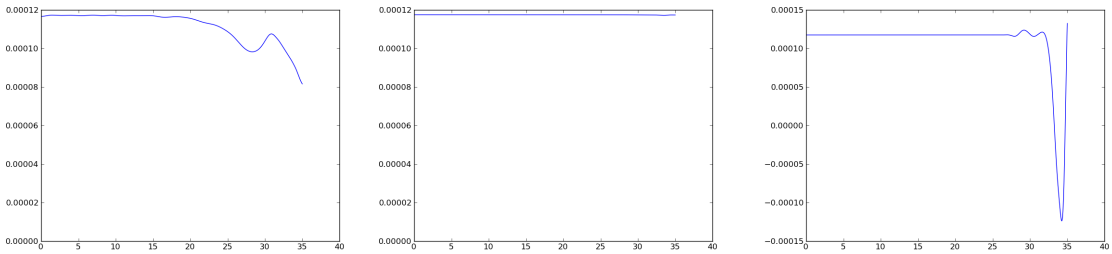

Figure 10: The relative error of energy for different degree of spline and with the second algorithm. To the left to right the degree of spline is equal to $1, 3$ and 5.

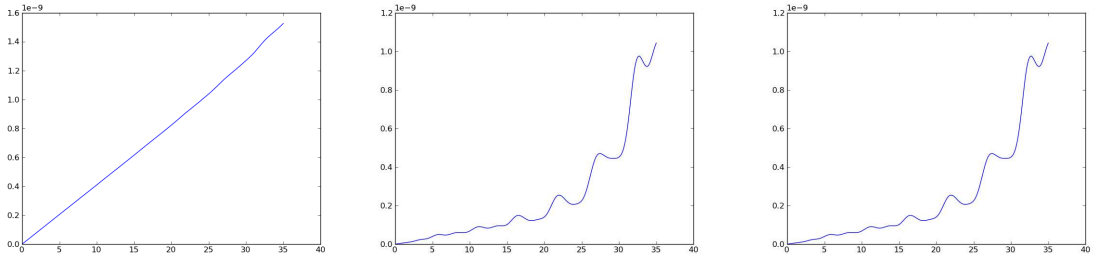

Figure 11: The relative error of momentum for different degree of spline with the first algorithm. To the left to right the degree of spline is equal to $1, 3$ and 5.

5. Conclusion

Spline discrete differential forms have been used to implement a Vlasov-Poisson solver. This is a first step towards a geometric discretisation of the Vlasov-Maxwell equations. Arbitrary high order in phase-space can be achieved easily, and the framework can be used to get discrete conservation properties as long as the full equation is solved not using split steps. However split step methods that consist only of 1D sweeps can be solved a lot faster, when a linear solver is involved as is the case for us. This is all the more true when going to more realistic phase-space dimensions which go up to 6

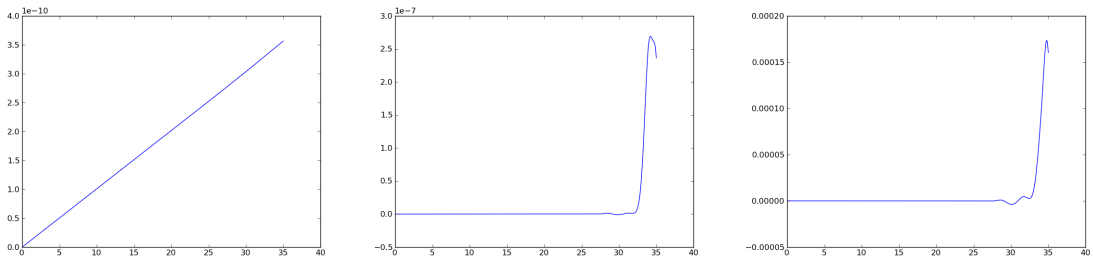

Figure 12: The relative error of momentum for different degree of spline with the second algorithm. To the left to right the degree of spline is equal to $1, 3$ and 5.

in real physics problems. Moreover they yield still very good conservation properties as was verified here.

References

[1] A. Back and E. Sonnendrücker, Discrete differential forms based on B-splines. Applications to Maxwell's equations (submitted).

[2] A. Back, Etude théorique et numérique des équations de Vlasov-Maxwell dans le formalisme covariant. Phd 2011.

[3] V.I. Arnold, Mathematical methods of classical mechanics, Graduate Texts in Mathematics, Springer-Verlag, New York, 1976.

[4] D.N. Arnold, R.S. Falk, R. Winther, Finite element exterior calculus, homological techniques, and applications, Acta Numerica 2006, pp. 1–155.

[5] R. Belaouar and N. Crouseilles and P. Degond and E. Sonnendrücker, An asymptotically stable semi-Lagrangian scheme in the quasi-neutral limit., J. Sci. Comput., 2009.

[6] N. Besse and M. Mehrenberger, Convergence of classes of high-order semi-Lagrangian schemes for the Vlasov-Poisson system, Math. Comp., 2008.

[7] A. Bossavit, Computational electromagnetism, Academic Press (Boston), 1998.

[8] A. Bossavit, Generating Whitney Forms of Polynomial Degree One and High, IEEE Trans. on Magnetics (2002), 341–344.

[9] A. Buffa and G. Sangalli and R. Vazquez, Isogeometric analysis in electromagnetics: B-splines approximation, Comput. Methods Appl. Mech. Engrg. 199 (2010), no. 17-20, 1143–1152

[10] A. Buffa and J. Rivas and G. Sangalli and R. Vázquez, Isogeometric discrete differential forms in three dimensions, SIAM Journal on Numerical Analysis, 2011, 49 no. 2, 818–844.

[11] S. M. Cox and P. C. Matthews, Exponential time differencing for stiff systems, J. Comput. Phys. 176, 430–455 (2002).

[12] N. Crouseilles, M. Mehrenberger and E. Sonnendrücker, Conservative semi-Lagrangian schemes for Vlasov equations, J. Comput. Phys., 2010.

[13] C. de Boor, A practical guide to splines, Revised edition. Applied Mathematical Sciences, 27. Springer-Verlag, New York, 2001.

[14] M. Desbrun, E. Kanso and Y. Tong , Discrete differential forms for computational modeling, Oberwolfach Semin. (2008), 287–324.

[15] M. Desbrun, M. Leok and J.E. Marsden, Discrete Poincaré lemma, Appl. Numer. Math. 53 no. 2 (2005), 231–248.

[16] F. Filbet and E. Sonnendrücker, Comparison of Eulerian Vlasov solvers, Computer Physics Communications, 150, 2003.

[17] R. Hiptmair, Finite elements in computational electromagnetism. Acta Numerica 11 (2002), 237–339.

[18] R. Hiptmair, Discrete Hodge operators. Numer. Math. 90 (2001), 265–289.

[19] F. Rapetti and A. Bossavit, Whitney forms of higher degree, SIAM J. Numer. Anal. 47 no. 3 (2009), 2369–2386.

[20] A. Ratnani and E. Sonnendrücker, Arbitrary High-Order Spline Finite Element Solver for the Time Domain Maxwell equations, J. Scientific Comput. 51 (1), 2012.

[21] E. Sonnendrücker, J. Roche, P. Bertrand and A. Ghizzo, The semi-Lagrangian method for the numerical resolution of the Vlasov equation, J. Comput. Phys., 1999.

[22] G. Manfredi, Long-time behavior of nonlinear Landau damping, Phys. Rev. Letters 79 (15), 2815–2818, 1997.

Appendix A. Equivalence between the Vlasov-Ampere equation and the Vlasov-Poisson equation in 1D

Lemma 1. *Let* (E, f) *be the solution of the Vlasov-Ampère equations* (3)–(4) *with* $\frac{\partial E}{\partial x}(x, 0) = \rho(x, 0)$. *Then* E *is solution of the Poisson equation* (5)

for all times.

Proof. Integrating the Vlasov equation (3) with respect to v yields the continuity equation

$$\frac{\partial \rho}{\partial t} + \frac{\partial J}{\partial x} = 0.$$

Then taking the x derivative of the Ampère equation and using this continuity equation we get

$$\frac{\partial^2 E}{\partial t \partial x} = -\frac{\partial J}{\partial x} = \frac{\partial \rho}{\partial t}.$$

Hence $\frac{\partial}{\partial t}(\frac{\partial E}{\partial x} - \rho) = 0$, and finally as $\frac{\partial E}{\partial x}(x,0) = \rho(x,0)$, this yields that the Poisson equation is satisfied for all times. ■

Lemma 2. *Let (E, f) be the solution of the Vlasov-Poisson equation* (3)–(5) *with $\int_0^L E(x,t)\,dx = 0$ for all times. Assume that $\int_0^L J(x,0)\,dx = 0$. Then E is solution of the Ampère equation* (4).

Proof. As for the previous lemma the proof is based on the continuity equation. Taking the time derivative of the Poisson equation and using this continuity equation we get

$$\frac{\partial^2 E}{\partial t \partial x} = \frac{\partial \rho}{\partial t} = -\frac{\partial J}{\partial x}.$$

Hence $\frac{\partial}{\partial x}(\frac{\partial E}{\partial t} + J) = 0$. Next multiplying the Vlasov equation by v and integrating over x and v, with an integration by parts in v on the last term, we get the conservation of total momentum

$$\frac{d}{dt}\int_0^L J(x,t)\,dx = \frac{d}{dt}\int_0^L f(x,v,t)v\,dx\,dv = \int_0^L \rho(x,t)E(x,t)\,dx$$
$$= \int_0^L \frac{\partial E}{\partial x} E\,dx = 0,$$

as E is periodic.

Finally as the average of J is initially 0, it stays so for all times and by hypothesis the average of E is also 0 for all times. This implies that the Ampère equation is verified.

$\blacksquare$